Chaos

AIP Publishing

Evolution of quasiperiodicity in quorum-sensing coupled identical Repressilators

N. Stankevich[1, a)] and E. Volkov[2]
[1)]*Laboratory of topological methods in dynamics, National Research University High School of Economics, Nizhny Novgorod, 25/12 Bolshay Pecherskaya str., Nizhny Novgorod 603155, Russia*[b)]
[2)]*2Department of Theoretical Physics, Lebedev Physical Institute, Moscow, 119991, Leninsky prospect, 53, Russia*

(Dated: 28 February 2020)

The dynamics of three three-dimensional Repressilators globally coupled by a quorum sensing mechanism was numerically studied. This number (three) of coupled Repressilators is a sufficient to obtain such a set of self-consistent oscillation frequencies of signal molecules in the mean field that results in the appearance of self-organized quasiperiodicity and its complex evolution over wide areas of model parameters. Analyzing numerically the invariant curves as a function of coupling strength, we observed torus doubling, three torus arising via quasiperiodic Hopf bifurcation, the emergence of resonant cycles, and secondary Neimark-Sacker bifurcation. A gradual increase in the oscillation amplitude leads to chaotizations of the tori and to the birth of weak, but multidimensional chaos.

Understanding the dynamic behavior of many real systems requires developing appropriate multidimensional models. Oscillator coupling is a quite popular way for constructing such models. Collective regimes can be very rich for a large set of coupling schemes even for identical oscillators. Population of bacterial cells with imbedded synthetic oscillators is a useful test bed for selecting the coupling schemes that lead to desirable sets of collective regimes. Coupling between genetic elements can be designed in a number of ways, of which bacterial quorum sensing (QS) seems to be a more natural one. Here, we investigate three globally coupled ring oscillators imitating the basic dynamic properties of the well-known synthetic genetic Repressilator. Our three-dimension version of Repressilator is a ring of three nonlinear elements (genes), whose protein products repress the transcription activity of each next gene in the ring unidirectionally, giving birth to soft oscillations. One element of each Repressilator produces signal molecules (autoinducer (AI)), which diffuse from cells, mixed fast in the environment and stimulate the activity of another element in the all three rings. In this way, one element of the ring is simultaneously a target of both repression and AI-dependent activation, which may generate remarkable multistability in the entire system. We focus on the evolution of quasiperiodicity generated via Neimark-Sacker bifurcation of a rotating wave if the coupling strength, which is controlled by autoinducer dilution in the environment, reaches a threshold. The enhancement of interactions leads to torus doubling, the formation of three tori via quasiperiodic Hopf bifurcation, the emergence of resonant cycles and secondary Neimark-Sacker bifurcation. Similar torus evolution has been presented in the literature for periodically stimulated limit cycles or coupled nonidentical oscillators but it is new for identical elements. A gradual increase in the oscillation amplitude leads to chaotization of the tori and to the birth of weak, but multidimensional chaos. Although some regimes have small areas of stability, their existence and transitions between them appear to be fundamentally important, and it is expected that they will manifest themselves more in the course of future work.

I. INTRODUCTION

Quasiperiodic oscillations are a kind of oscillations characterized by two or more incommensurable frequencies. This class of oscillations is found in many areas of science and technology[1,2]. Quasiperiodicity in oscillating systems can be implemented in many ways. As a rule, quasi-periodic oscillations are associated with non-identity in the ensemble of oscillators with attractive connections. For a slight detuning in frequency or other parameters, in-phase synchronization is observed. With an increase in detuning the limit cycles disappear and quasi-periodic modes emerge via a saddle-node bifurcation[3]. In the parameter plane, one can observe typical Arnold tongues surrounded by quasi-periodic regimes. In systems with a large number of incommensurable frequencies, variation of the parameters responsible for nonidentity leads to the formation of the Arnold resonance web[4].

Autonomous four-[5] and three-[6,7] dimensional radiophysical quasiperiodic oscillators were constructed by addition of slow relaxation variables to the classical two dimensional oscillators. Multi-frequency quasiperiodic oscillations have been attracting interest from researchers since the time that turbulence was described in the Landau-Hopf scenario by involving additional frequencies in the dynamics of the system[8]. Multi-frequency tori were shown to persist and evolve in sufficiently large regions of the parameter space[9,10]. The main robust tool to uniquely diagnose tori is to find the spectrum of Lyapunov exponents[11]. For systems with a large-

[a)]Electronic mail: stankevichnv@mail.ru.
[b)]Also at Department of Radio-Electronics and Telecommunications, Yuri Gagarin State Technical University of Saratov, 77 Politekhnicheskaya str., Saratov 410054, Russia.; Also at Department of Applied Cybernetics, St. Petersburg State University, Saint-Petersburg, Peterhof, 28 Universitetskiy proezd, St. Petersburg 198504, Russia

dimension phase space, calculating the full spectrum of Lyapunov exponents is a challenging task. The development of computing power has led to a new surge of interest in systems with multi-frequency quasiperiodic dynamics[12–19].

Bifurcations of tori were classified as the saddle-node, Hopf, and torus doubling types[12,13]. Various bifurcation mechanisms of the transition from two-frequency to three-frequency quasiperiodic dynamics were investigated[14–16]. The synchronous regimes in the periodically forced resonant limit cycle on a torus[17], in coupled multimode oscillators with time-delayed feedback[18], and coupled autonomous quasiperiodic generators[19] were examined. Analysis of torus-doubling bifurcations for three and four dimension maps started many years ago by Kaneko[20,21] was recently performed for the simplest 4D model of a real radio-physical generator[5].

At present, special attention is paid to the routes toward various types of chaos from torus. An interesting scenario leading to hyperchaos through two-frequency torus destruction caused by a sequence of secondary Neimark-Sacker bifurcations is found in two coupled anti-phase excited Toda oscillators[22], in the dynamical system with a minimal dimension of phase space, 4D radio-physical oscillator[23], and in the model of two coupled contrast agents that are gas bubbles encapsulated into a viscoelastic shell[24]. Another scenario describes the development of chaos with an additional zero Lyapunov exponent in the spectrum as a result of a cascade of invariant curve doubling bifurcations in two coupled quasiperiodic generators[19].

In papers[25–27], the concept of self-organized quasiperiodicity was introduced. The distinctive property of self-organized quasi-periodicity is that it occurs in ensembles of all-to-all coupled *identical* oscillators due to nonlinear dependence of coupling on the order parameters.

In the last decade the coupling schemes inspired by quorum sensing (QS) signaling mechanism, whereby bacteria communicate in a growing population, are increasingly used in the studies of collective behavior in different systems, e.g., chemical oscillators[28], glycolytic oscillations in yeast[29], coupled lasers[30], chaotic oscillators[31]. In these publications only the population density is the key parameter that controls the dynamics of signal molecules but no particular attention was given to the choice of their targets in the interacting oscillators.

For QS-coupled synthetic genetic oscillators embedded in bacteria the production of signal molecules (autoinducers) may be realized as an additional process which is correlated with the expression of one gene in the genetic circuit that may differ from the target gene[32,33]. This flexibility of the coupling design opens new possibilities both for the generation of coherent behavior in heterogeneous populations[32,33] and for the remarkable variability of collective regimes in homogeneous ones. Self-organized Quasiperiodic dynamics were found[34,35] in the system of two QS-coupled identical ring oscillators (Repressilators)[36]. For this system the two-frequency torus formation is the starting event for the development of flexible dynamics over the extended areas of the parameter space. An increase in the number of interacting oscillators complicates the dynamics of the system and can lead to the emergence of new types of behavior. Here we investigate the evolution of quasiperiodicity in the three identical mean-field QS-coupled Repressilators. Just this kind of coupling implemented in three-dimensional oscillators provides a new scenario for torus evolution.

We demonstrate torus doubling bifurcations for all values of the maximum transcription rate tested and over extended intervals of coupling strengths, as well as three-frequency torus emergence via quasiperiodic Hopf bifurcation (however, the parameter intervals of its stability are quite limited because of its transition to weak chaos). We found also a small spot of parameters (the maximum transcription rate versus the coupling strength) where the resonant cycle undergoes secondary Neimark-Sacker bifurcation and transforms to 11-turn two-frequency torus and returns to chaos. The emergence of chaotic regimes with different spectra of Lyapunov exponents are also found.

The work is structured as follows. In Sect. II, we describe the model, the main model parameters, methods for studying the regions in the parameter space where various quasiperiodic regimes may exist, and then examine the mechanism whereby a two-frequency torus arises. In Sect. III, a detailed numerical study of the dynamics of the system is given, with the focus on the evolution of quasiperiodic oscillations (bifurcation of the torus, its destruction).

II. SYSTEM OVERVIEW

As the basis we use a reduced version of the model described earlier (see[37] for details) and adapted for three three-dimensional Repressilators coupled via autoinducer production and diffusion. Figure 1 shows three Repressilators located

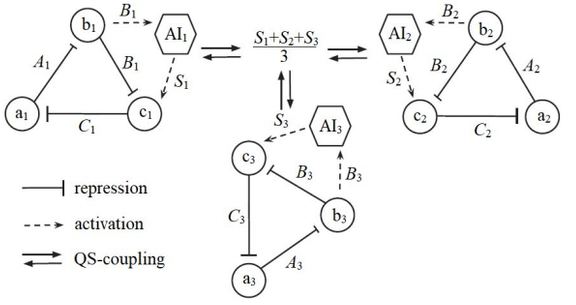

FIG. 1. Principle scheme of three quorum-sensing coupled Repressilators. A_i, B_i, C_i are proteins in each Repressilators; a_i, b_i, c_i are mRNAs produced by three genes; AI_i are autoinducers and S_i are their concentrations.

in different cells (or other appropriate containers impermeable to repressors) and coupled by QS exchange via the external medium. The three genes in the ring produce mRNAs (a, b, c) which are translated to proteins (A, B, C), and they impose Hill function inhibition on each next gene in the ring (each ring member is inhibited by the preceding one and, in its turn, inhibits the next one). The QS feedback is maintained by the AI produced (rate k_{S1}) proportionally to the protein B con-

centration while the autoinducer (AI) communicates with the environment and activates the production of mRNA for protein C (rate κ in combination with Michaelis function), which, in turn, reduces protein A concentration, thereby stimulating protein B production. In this way protein B plays a dual role of direct inhibition of protein C synthesis and AI-dependent activation of protein C synthesis, resulting in the complex dynamics of the Repressilator, even for a single Repressilator[38]. Eventually, the equations for dimensionless repressors (A, B, C) and autoinducer (S) concentrations are:

$$\begin{aligned}
\dot{A}_i &= \beta_1(-A_i + \tfrac{\alpha}{1+C_i^n}),\\
\dot{B}_i &= \beta_2(-B_i + \tfrac{\alpha}{1+A_i^n}),\\
\dot{C}_i &= \beta_3(-C_i + \tfrac{\alpha}{1+B_i^n} + \tfrac{\kappa S_i}{1+S_i}),\\
\dot{S}_i &= -k_{S0}S_i + k_{S1}B_i - \eta(S_i - S_{ext}),
\end{aligned} \tag{1}$$

where $i = 1,2,3$ are subscripts for the three Repressilators, β_j ($j = 1,2,3$) are the ratios of the protein decay rate to the mRNA decay rate, α stands for the maximum transcription rate in the absence of the inhibitor, and n is the Hill cooperativity coefficient for inhibition. For the quorum sensing pathway k_{S0} is the ratio of the S decay rate to the mRNA decay rate, and, as previously mentioned, k_{S1} is the S production rate, (κ is a measure of S-dependent activation of protein C production. The diffusion coefficient η depends on the membrane permeability to the S molecule. The autoinducer concentration in the external medium S_{ext} is determined (in a quasi-steady state approximation) by S_i produced by all the Repressilators (S_1, S_2, S_3) and a dilution factor Q:

$$S_{ext} = Q\frac{S_1 + S_2 + S_3}{3}. \tag{2}$$

The model parameters are fixed identical for each Repressilator and close to what was proposed in[37]: $\beta_1 = 0.5$, $\beta_2 = \beta_3 = 0.1$, $n = 3$, $k_{S0} = 1$, $k_{S1} = 0.01$, $\eta = 2$, $\kappa = 15$. As a control parameter, we use the coupling strength Q and the maximum transcription rate in the absence of inhibitor α.

At $Q = 0$, each Repressilator demonstrates non-stiff self-oscillations. In a system of three Repressilators with a low coupling strength, the time series of the limit cycle are presented in Fig. 2 for $\alpha = 230$, $Q = 0.5$. Figure 2a shows the time realizations of each variable A, B, C of one Repressilator: the amplitudes of the repressors are different due to the presence of QS feedback. Figure 2b shows the time series of the A-repressors in each of the three coupled oscillators: as a result of the identity of the oscillators, they have the same amplitudes, but each of the time realization is shifted by one third of the period relative to the next. Such a solution in the literature is frequently called a rotating wave (RW) see e.g.[39,40]. **Although $\beta_i < 1$, their values are not small enough to permit mathematically correct reduction of the linear differential equations for S_i. However, we can calculate S_i in a quasi-steady state approximation ($dS_i/dt = 0$) in order to get qualitative formulae for S_i as functions of variables B_i:**

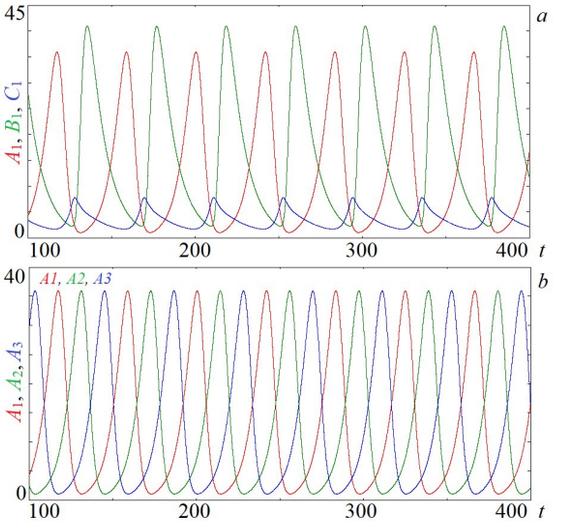

FIG. 2. (a) Time series of all variables (A, B, C) for one of the three coupled Repressilators and (b) time series of the variables A_1, A_2, A_3 for small coupling strength $Q = 0.5$. Other parameters are: $\beta_1 = 0.5$, $\beta_2 = \beta_3 = 0.1$, $n = 3$, $k_{S0} = 1$, $k_{S1} = 0.01$, $\eta = 2$, $\kappa = 15$, $\alpha = 230$, $Q = 0.5$.

$$\begin{aligned}
S_1 &= 1/3 * (k_{S1}(B_1 + B_2 + B_3)/(k_{S0} + \eta - \eta * Q) -\\
&-k_{S1}(2B_1 - B_2 - B_3)/(k_{S0} + \eta),\\
S_2 &= 1/3 * (k_{S1}(B_1 + B_2 + B_3)/(k_{S0} + \eta - \eta * Q) -\\
&-k_{S1}(2B_2 - B_1 - B_3)/(k_{S0} + \eta),\\
S_3 &= 1/3 * (k_{S1}(B_1 + B_2 + B_3)/(k_{S0} + \eta - \eta * Q) -\\
&-k_{S1}(2B_3 - B_1 - B_2)/(k_{S0} + \eta).
\end{aligned} \tag{3}$$

These expressions show several combinations of B_i that stimulate the production of variables C_i. In the presence of inescapable phase differences between B_i oscillations such oscillating stimulation terms in the equations for C_i may contain many frequencies giving rise to quasiperiodicity and other collective regimes (see Results in Sect.III) for three coupled identical oscillators. As the coupling strength Q increases, the Neimark-Sacker bifurcation converts the rotating wave to a two-frequency torus. In this work, we keep parameter α in the range of 150-300 to focus on the torus evolution without the influence of other regimes that may appear, as we know from the previous studies, with oscillator's amplitude growth. Figure 3 shows the two-parameter chart of the dynamic modes and the chart of Lyapunov exponents, on which the domains of existence of various dynamic modes are marked with different colors. The Lyapunov exponent chart was constructed as follows: for each point of the parameter plane, the full spectrum of Lyapunov exponents was calculated using the Benettin algorithm and Gram-Schmidt orthogonalization[41]. Depending on the values of Lyapunov exponents the dynamic mode was diagnosed. When constructing a chart of dynamic modes for each point of the parameter plane, we analyzed the number of fixed points in the Poincaré section with the hypersurface $C_1 = 5$. The chart of dynamic modes makes it possible to distinguish between periodic and

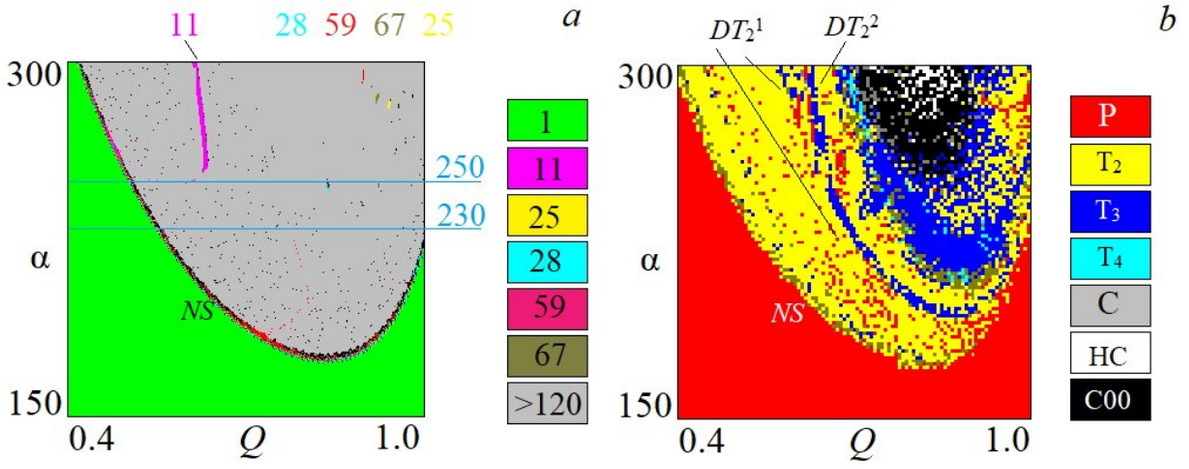

FIG. 3. Structure of the parameter plane (Q, α) for three coupled Repressilators (1), $\beta_1 = 0.5$, $\beta_2 = \beta_3 = 0.1$, $n = 3$, $k_{S0} = 1$, $k_{S1} = 0.01$, $\eta = 2$, $\kappa = 15$: (a) chart of dynamical modes, different colors marked different periods of self-oscillations in accordance with numbers in rectangles; (b) chart of Lyapunov exponents. *NS* is the line of Neimark-Sacker bifurcation; DT_2^1, DT_2^2 are lines of torus doubling bifurcations.

non-periodic oscillations, as well as to present the values of period for periodic oscillations (the palette next to the chart). The chart of Lyapunov exponents reveals the parameter intervals with many periodic modes and allows various quasiperiodic and chaotic ones to be classified in accordance with the following notation (the palette is also presented in Fig. 3b):

- periodic (P), $\Lambda_1 = 0$, $0 > \Lambda_2 > \Lambda_3 > \Lambda_4 > \Lambda_5 > \Lambda_6$;
- quasiperiodic two-frequency (T_2), $\Lambda_1 = \Lambda_2 = 0$, $0 > \Lambda_3 > \Lambda_4 > \Lambda_5 > \Lambda_6$;
- quasiperiodic three-frequency (T_3), $\Lambda_1 = \Lambda_2 = \Lambda_3 = 0$, $0 > \Lambda_4 > \Lambda_5 > \Lambda_6$;
- chaotic (C), $\Lambda_1 > 0$, $\Lambda_2 = 0$, $0 > \Lambda_3 > \Lambda_4 > \Lambda_5 > \Lambda_6$;
- chaotic with an additional zero Lyapunov exponent (C00), $\Lambda_1 > 0$, $\Lambda_2 = \Lambda_3 = 0$, $0 > \Lambda_4 > \Lambda_5 > \Lambda_6$, (Quasiperiodic Henon attractor[42]);
- hyperchaotic (HC), $\Lambda_1 > \Lambda_2 > 0$, $\Lambda_3 = 0$, $0 > \Lambda_4 > \Lambda_5 > \Lambda_6$.

The dynamics of the Lyapunov exponents as a function of the parameter may classify some bifurcations of quasiperiodic oscillations[12]. The two-frequency torus doubling bifurcation can be described by the following dependence of the three largest Lyapunov exponents on the parameter: before the bifurcation the two largest Lyapunov exponents are equal to zero and the third one is negative; at the moment of bifurcation, the third largest exponent also becomes zero; after the bifurcation the third largest Lyapunov exponent again becomes negative, while the other two remain unchanged (zero). In accordance with the classification proposed above, we observe the appearance of thin lines indicating the location of a torus doubling bifurcations inside the region of the two-frequency torus in the parameter plane (DT_2^1, DT_2^2 in Fig. 3b).

The parameter plane is bounded by line $Q = 1$, which corresponds to the relevant maximal values of the coupling strength. On the charts, the Neimark-Sacker (*NS*) bifurcation line is clearly visible (Fig. 3a), it has a parabola-like shape which demonstrates the reverse Neimark-Sacker bifurcation and returning the Repressilators to periodic self-oscillations at sufficiently large values of parameter Q. With increasing α the destruction of quasiperiodic oscillations gives rise to chaotic dynamics. An interesting detail is that, according to the spectrum of Lyapunov exponents, three types of chaotic dynamics can be distinguished. However, the dominant type of chaotic behavior is chaos with an additional zero Lyapunov exponent. On the chart of the dynamic regimes inside the two-frequency torus domain, narrow tongues with periodic regimes are visible. Their distinctive feature is that they have a very large period and occupy small areas in the parameter plane compared with the resonant cycles found in two coupled Repressilators[37]. For a given accuracy it is possible to identify the tongues with periods of 11, 28, 59, 67, 25 limit cycles and to observe period doubling bifurcations for cycles with periods of 28 and 25. Several limit cycles are important below for the study of torus evolution but as a whole the role of such cycles in dynamics of three Repressilators is beyond the current work.

The bifurcation lines of two-frequency torus doubling (DT_2^1, DT_2^2), the formation of a three-frequency torus, and also the destruction of torus with the formation of a chaotic attractor are observed. In the next Section, the transformation of quasiperiodic oscillations will be considered in detail.

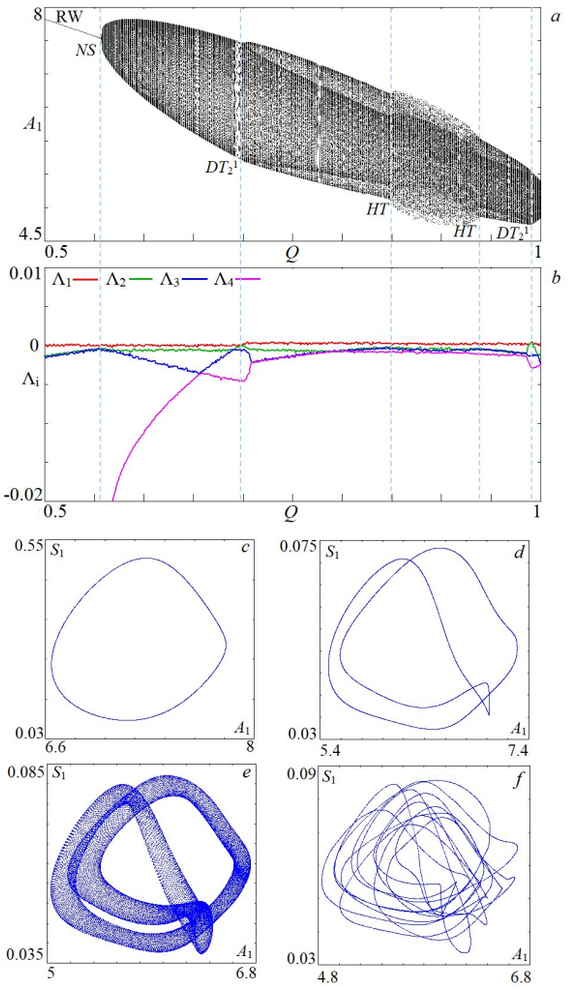

FIG. 4. (a) bifurcation diagram, (b) plots of the four largest Lyapunov exponents and (c) -(e) two-dimensional projections in the Poincaré section by hypersurface $C_1 = 5.0$. $\beta_1 = 0.5$, $\beta_2 = \beta_3 = 0.1$, $n = 3$, $k_{S0} = 1$, $k_{S1} = 0.01$, $\eta = 2$, $\kappa = 15$, $\alpha = 230$; c) $Q = 0.6$; d) $Q = 0.75$; e) $Q = 0.85$; f) $Q = 0.87$. *NS* is Neimark-Sacker bifurcation, DT_2^1 is torus doubling bifurcations, *HT* is quasi-periodic Hopf bifurcations.

III. RESULTS. EVOLUTION OF QUASI-PERIODIC DYNAMICS

A. $\alpha = 230$

First, we choose a value of parameter α that corresponds to a domain in the chart of Lyapunov exponents (Fig. 3) where three-frequency quasiperiodic oscillations are observed, say, $\alpha = 230$. Figure 4 shows the bifurcation tree (Fig. 4a) and the graphs of the four largest Lyapunov exponents (Fig. 4b) for $\alpha = 230$ versus the coupling parameter Q. Figures 4c - 4f present all the identified, qualitatively different two-dimensional projections of the characteristic phase portraits in the Poincaré section with the hypersurface $C_1 = 5$. The letters on the bifurcation tree indicate the main bifurcations determined based on the invariant curves type, and the spectrum of Lyapunov exponents (if this spectrum allows clear identification).

At $\alpha = 230$ the anti-phase RW loses stability as Q increases and a two-frequency torus is born via Neimark-Sacker bifurcation. Further torus evolution includes its doubling (DT_2^1), which is clearly visible in the phase portraits: a one-turn invariant curve (Fig. 4c) becomes a two-turn one (Fig. 4d). Then, on the basis of the doubled torus, as a result of quasiperiodic Hopf bifurcation (*HT*), a three-frequency torus arises, its phase portrait is shown in Fig. 4e. With a further increase in Q, a partial locking of one of the frequencies can be observed: a multi-turn two-frequency torus appears on the surface of the three-frequency torus as can be seen in Fig. 4f. At large Q values the inverse quasiperiodic Hopf bifurcation takes place: the three-frequency torus transforms into a two-turn two-frequency torus. Thereafter, the reverse bifurcation of torus doubling occurs, i.e. the two-turn invariant curve transforms into one-turn invariant curve (not shown in Fig. 4). Thus, for $\alpha = 230$ and varied coupling strength, two types of bifurcations of invariant curves are observed; however, no chaotic dynamics develops.

B. $\alpha = 250$

At somewhat larger α weak chaotic oscillations develop during torus evolution. Figure 5 shows the bifurcation tree, the four largest Lyapunov exponents and the set of two-dimensional projections of phase portraits in the Poincaré section for $\alpha = 250$.

At the start, the scenario coincides with that for $\alpha = 230$: the smooth invariant curve in Fig. 5c sets in from the Neimark-Sacker bifurcation of RW. As Q increases, the invariant curve shape becomes more complex. Shown in Fig. 5d is the invariant curve on which an additional loop appears without bifurcation. Thereafter, a two-turn invariant curve arises as a result of the torus doubling bifurcation (DT_2^1) (Fig. 5e), followed by a next torus doubling bifurcation (DT_2^2) (Fig. 5f). This four-turn invariant curve does not demonstrate further complication but instead the system does step back by the inverse torus doubling bifurcation (Fig. 5g).

Starting from the doubled torus, a three-frequency torus appears as a result of quasiperiodic Hopf bifurcation (*HT*) (Fig. 5h). Figures 5i and 5j depict the two-frequency regimes arising on the surface of the three-frequency torus. Obviously, the invariant curve becomes more complex. After that, the three-frequency torus tends to collapse (Figs. 5k, 5m). The phase points are distributed over the three-frequency torus surface; however, they condense in the vicinity of the invariant curves corresponding to the two-frequency torus. In this case, double-frequency tori corresponding to partial frequency locking can still appear on the three-frequency torus surface (Fig. 5l). The final destruction of the three-frequency torus leads to the formation of a chaotic attractor, which is seen as a diffuse cloud of phase points without definite structure (Fig. 5n).

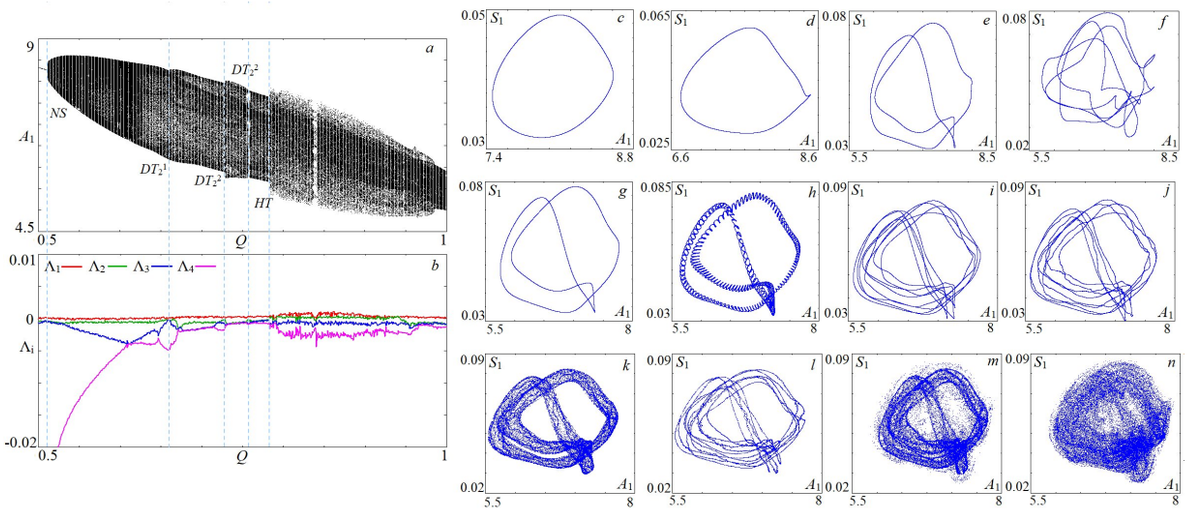

FIG. 5. (a) bifurcation diagram, (b) plots of the four largest Lyapunov exponents and (c) - (n) two-dimensional projections in the Poincaré section by hypersurface $C_1 = 5.0$. $\beta_1 = 0.5$, $\beta_2 = \beta_3 = 0.1$, $n = 3$, $k_{S0} = 1$, $k_{S1} = 0.01$, $\eta = 2$, $\kappa = 15$, $\alpha = 250$; c) $Q = 0.54$; d) $Q = 0.6$; e) $Q = 0.72$; f) $Q = 0.73$; g) $Q = 0.76$; h) $Q = 0.78$; i) $Q = 0.7802$; j) $Q = 0.782$; k) $Q = 0.7821$; l) $Q = 0.7823$; m) $Q = 0.7826$; n) $Q = 0.7827$. *NS* is Neimark-Sacker bifurcation, DT_2^1, DT_2^2 are torus doubling bifurcations, *HT* is quasi-periodic Hopf bifurcation.

C. $\alpha = 300$

A further increase in α causes the oscillation amplitude to grow and broadens the coupling strength intervals where tori get doubled. Figures 6a and 6b demonstrate a bifurcation tree, a graph of the four largest Lyapunov exponents for $\alpha = 300$. Three lines of torus doubling bifurcations are indicated on the bifurcation tree and graphs of Lyapunov exponents (DT_2^1, DT_2^2, DT_2^3) (Fig. 6a, 6b). Figures 6c -6j show the phase portraits for $\alpha = 300$, starting from the Q values at which torus doubling has already occurred twice (Fig. 6c). Thereafter torus destruction is observed: regions of local instability appear on its invariant curves, which begin to merge and intersect (Fig. 6d). A further increase in Q causes the invariant curves to transform into bands, inside which the phase points are distributed fairly uniformly. The bands corresponding to different invariant curves expand and merge, forming a chaotic attractor shown in Fig. 6f. This transformation of the attractor in the Poincaré sections is typical of the special chaotic attractors with an additional zero exponent in the spectrum of Lyapunov exponents[19,42]. The formation of such chaotic attractors occurs if a chaotic attractor absorbs saddle tori resulting from a cascade of torus doubling bifurcations or their homoclinic bifurcation.

The next dynamic event is the appearance of a long-period limit cycle with 11:11:11 winding number (LC^{11} in Fig. 6g). On the basis of this cycle, the secondary Neimark-Sacker bifurcation (NS^{11})[22–24] occurs, and in the vicinity of each fixed point in the Poincaré section there appears an invariant curve (Fig. 6h). In this way, 11 invariant curves arise in the Poincaré section, which corresponds to an 11-turn two-frequency torus stable over quite a short Q-interval. As Q increases the 11-turn double-frequency torus doubles, as can be seen in Fig. 6i. In total, it is possible to track two doubling bifurcations before a chaotic attractor with an additional zero Lyapunov exponent arises (Fig. 6j), as it is observed for the two-turn invariant curve (Fig. 6f). Then the chaotic attractors, which consist of 11 "islands" corresponding to the basic invariant curves, join together and transform back into a two-turn invariant curve and a new coupling-dependent evolution of complex dynamics begins from the newborn chaos starting at $Q = 0.69$.

TABLE I. Signature of the spectrum of the Lyapunov exponents for chaotic attractors, $\beta_1 = 0.5$, $\beta_2 = \beta_3 = 0.1$, $n = 3$, $k_{S0} = 1$, $k_{S1} = 0.01$, $\eta = 2$, $\kappa = 15$, $\alpha = 300$.

Q	Λ_1	Λ_2	Λ_3	Λ_4	Λ_5
0.7	0.0015	0.0	-0.0007	-0.0031	-0.0392
0.8	0.0032	0.0008	0.0	-0.0026	-0.0345

At even higher Q values a new start for complex dynamics development is observed. Figure 7 illustrates various representative chaotic attractors by their phase portraits in the Poincaré section. Long-period resonant cycles (see e.g. LC^{21} in Fig. 7a) emerge on the torus surface and then break down, resulting in the rugged invariant curve (Fig. 7b). The attractor structure becomes more blurred (see Figs. 7c, 7d), with the attractors four largest Lyapunov exponents going very close to zero in the interval between lines C_1 and C_2 in Figs. 6a, 6b. Mature chaos evolution is shown in Figs. 7e, 7f (lines C_2-C_3 in Figs. 6a, 6b) as a process of portrait structure breakdown to a nearly uniform cloud of phase points. Interestingly, this attractor has two small but positive and one zero Lyapunov exponents (see Table I), which may indicate possible emergence of hyperchaos. This possibility will be addressed in future studies.

For $\alpha = 300$, similar to what was observed for $\alpha =$

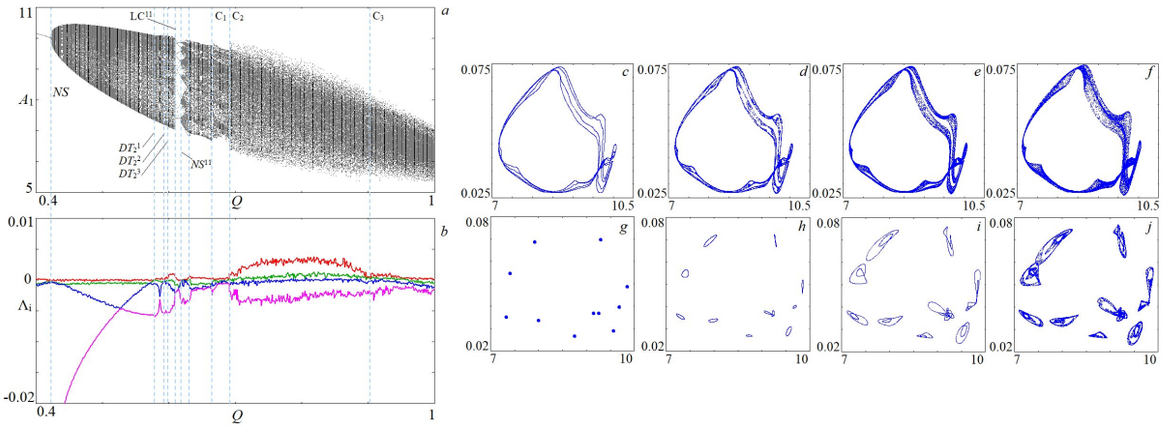

FIG. 6. (a) bifurcation diagram, (b) plots of the four largest Lyapunov exponents and (c) - (j) two-dimensional projections in the Poincaré section by hypersurface $C_1 = 5.0$. $\beta_1 = 0.5$, $\beta_2 = \beta_3 = 0.1$, $n = 3$, $k_{S0} = 1$, $k_{S1} = 0.01$, $\eta = 2$, $\kappa = 15$, $\alpha = 300$; c) $Q = 0.596$; d) $Q = 0.5965$; e) $Q = 0.597$; f) $Q = 0.6$; g) $Q = 0.6185$; h) $Q = 0.62$; i) $Q = 0.6225$; j) $Q = 0.623$. *NS* is Neimark-Sacker bifurcation, DT_2^1, DT_2^2, DT_2^3 are torus doubling bifurcations, LC^{11} is occurrence of the limit cycle with winding number 11:11:11; NS^{11} is Neimark-Sacker bifurcation on the base cycle 11:11:11.

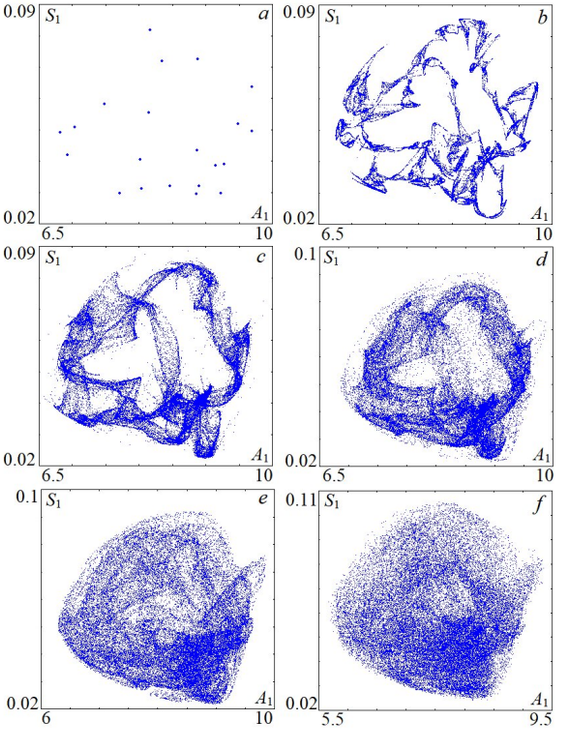

FIG. 7. Two-dimensional projections in the Poincaré section by hypersurface $C_1 = 5.0$. $\beta_1 = 0.5$, $\beta_2 = \beta_3 = 0.1$, $n = 3$, $k_{S0} = 1$, $k_{S1} = 0.01$, $\eta = 2$, $\kappa = 15$, $\alpha = 300$; a) $Q = 0.666$; b) $Q = 0.67$; c) $Q = 0.6803$; d) $Q = 0.69$; e) $Q = 0.7$; f) $Q = 0.8$.

230,250, in the high-Q region the dynamics complexity is gradually reduced and the system evolution terminates via the following events: chaos, doubled torus, two-frequency torus and rotating wave.

IV. CONCLUSION

Evolution of quasiperiodicity in ensembles of interconnected identical oscillators has not received much attention so far because there are just a few coupling schemes leading to torus formation. To the best of our knowledge the self-organized quasiperiodicity, as a typical regime in such systems, was found in[25,34] only. Indirect coupling of oscillators via production and fast diffusion of special signal molecules is a widespread phenomenon in the oscillator populations of different nature. In particular, the well-known interbacterial interactions suggest a mechanism (quorum sensing) that can be used to develop many coupling schemes for oscillators of different nature.

Many models of coupled synthetic genetic oscillators are not motivated purely for direct application to real experiments. Instead, they are developed as tools for revealing the potential range of dynamics for these coupled oscillators. For instance, models[32,33] demonstrated the principle possibility of full in-phase synchronization in detuned genetic oscillators, while coupling of identical relaxation oscillators in[43] opened the appearance of the inhomogeneous steady state.

We studied numerically the dynamics generated by one of such schemes in three coupled identical three-dimensional ring oscillators constructed by analogy to the synthetic genetic Repressilator[36]. According to system (1), the quorum sensing mechanism forms the mean field concentration of autoinducers, which can have the parameter-dependent set of frequencies incommensurate with those of the oscillators. In other words, under the chosen type of QS-coupling three oscillators with identical periods for $Q = 0$ may run along a two-frequency torus instead of the rotating wave-type limit cycle. We traced the evolution of the two-frequency torus over the whole interval of possible coupling strengths ($Q < 1$) and for several values of α (parameter controlling the oscillation am-

plitude). The first phenomenon detected is torus doubling observed for all α tested and over extended intervals of coupling strengths. The next effect is the three-frequency torus formation via quasiperiodic Hopf bifurcation; however, the parameter intervals of its stability are quite limited because of its transition to weak chaos. We found also a small spot of parameters ($\alpha - Q$) where the resonant cycle (11:11:11) is formed on the torus but then converts to 11-turn torus via Neimark-Sacker bifurcation and returns to chaos. Although this area is small for given values of α, the principle possibility of such transitions seems important. At last, but not least, the emergence of chaotic regimes with different spectra of Lyapunov exponents, including that with additional zero, as well as the spectrum with two positive exponents, are also found.

The QS coupling in the form fixed in system (1) is not specific to bacterial communication and may be realized in radiophysical networks, in coupled chemical oscillators etc. Further studies of the dynamics evolution in such systems over extended areas of parameters are likely to be rewarding in terms of discovering the route to hyperchaos.

ACKNOWLEDGMENTS

This work was supported by the grant of Russian Foundation for Basic Research (project No. 19-02-00610)

CONFLICT OF INTEREST

The authors declare that they have no conflict of interest.

[1] P. S. Landa, *Nonlinear oscillations and waves in dynamical systems*, Vol. 360 (Springer Science & Business Media, 2013).
[2] V. S. Anishchenko, T. Vadivasova, and G. Strelkova, *Deterministic nonlinear systems*, Vol. 294 (Switzerland: Springer International Publishing, 2014).
[3] A. Balanov, N. Janson, D. Postnov, and O. Sosnovtseva, *Synchronization: from simple to complex* (Springer Science & Business Media, 2008).
[4] C. Froeschlé, M. Guzzo, and E. Lega, "Graphical evolution of the arnold web: from order to chaos," Science **289**, 2108–2110 (2000).
[5] V. Anishchenko and S. Nikolaev, "Generator of quasi-periodic oscillations featuring two-dimensional torus doubling bifurcations," Technical physics letters **31**, 853–855 (2005).
[6] A. Kuznetsov, S. Kuznetsov, E. Mosekilde, and N. Stankevich, "Generators of quasiperiodic oscillations with three-dimensional phase space," The European Physical Journal Special Topics **222**, 2391–2398 (2013).
[7] N. Stankevich and E. Volkov, "Multistability in a three-dimensional oscillator: tori, resonant cycles and chaos," Nonlinear Dynamics **94**, 2455–2467 (2018).
[8] L. D. Landau, "On the problem of turbulence," in *Dokl. Akad. Nauk USSR*, Vol. 44 (1944) p. 311.
[9] H.-T. Moon, P. Huerre, and L. Redekopp, "Three-frequency motion and chaos in the ginzburg-landau equation," Physical Review Letters **49**, 458 (1982).
[10] N. Stankevich, A. Kuznetsov, and E. Seleznev, "Quasi-periodic bifurcations of four-frequency tori in the ring of five coupled van der pol oscillators with different types of dissipative coupling," Technical Physics **62**, 971–974 (2017).
[11] A. Pikovsky and A. Politi, *Lyapunov exponents: a tool to explore complex dynamics* (Cambridge University Press, 2016).
[12] R. Vitolo, H. Broer, and C. Simó, "Quasi-periodic bifurcations of invariant circles in low-dimensional dissipative dynamical systems," Regular and Chaotic Dynamics **16**, 154–184 (2011).
[13] M. Komuro, K. Kamiyama, T. Endo, and K. Aihara, "Quasi-periodic bifurcations of higher-dimensional tori," International Journal of Bifurcation and Chaos **26**, 1630016 (2016).
[14] N. Inaba, M. Sekikawa, Y. Shinotsuka, K. Kamiyama, K. Fujimoto, T. Yoshinaga, and T. Endo, "Bifurcation scenarios for a 3d torus and torus-doubling," Progress of Theoretical and Experimental Physics **2014** (2014).
[15] S. Hidaka, N. Inaba, K. Kamiyama, M. Sekikawa, and T. Endo, "Bifurcation structure of an invariant three-torus and its computational sensitivity generated in a three-coupled delayed logistic map," Nonlinear Theory and Its Applications, IEICE **6**, 433–442 (2015).
[16] M. Sekikawa and N. Inaba, "Doubly twisted neimark–sacker bifurcation and two coexisting two-dimensional tori," Physics Letters A **380**, 171–176 (2016).
[17] V. Anishchenko, S. Nikolaev, and J. Kurths, "Peculiarities of synchronization of a resonant limit cycle on a two-dimensional torus," Physical Review E **76**, 046216 (2007).
[18] Y. P. Emelianova, V. V. Emelyanov, and N. M. Ryskin, "Synchronization of two coupled multimode oscillators with time-delayed feedback," Communications in Nonlinear Science and Numerical Simulation **19**, 3778–3791 (2014).
[19] A. Kuznetsov, S. Kuznetsov, N. Shchegoleva, and N. Stankevich, "Dynamics of coupled generators of quasiperiodic oscillations: Different types of synchronization and other phenomena," Physica D: Nonlinear Phenomena **398**, 1–12 (2019).
[20] K. Kaneko, "Doubling of torus," Progress of theoretical physics **69**, 1806–1810 (1983).
[21] K. Kaneko, "Oscillation and doubling of torus," Progress of theoretical physics **72**, 202–215 (1984).
[22] N. V. Stankevich, A. Dvorak, V. Astakhov, P. Jaros, M. Kapitaniak, P. Perlikowski, and T. Kapitaniak, "Chaos and hyperchaos in coupled antiphase driven toda oscillators," Regular and Chaotic Dynamics **23**, 120–126 (2018).
[23] N. Stankevich, A. Kuznetsov, E. Popova, and E. Seleznev, "Chaos and hyperchaos via secondary neimark–sacker bifurcation in a model of radiophysical generator," Nonlinear Dynamics **97**, 2355–2370 (2019).
[24] I. R. Garashchuk, D. I. Sinelshchikov, A. O. Kazakov, and N. A. Kudryashov, "Hyperchaos and multistability in the model of two interacting microbubble contrast agents," Chaos: An Interdisciplinary Journal of Nonlinear Science **29**, 063131 (2019).
[25] M. Rosenblum and A. Pikovsky, "Self-organized quasiperiodicity in oscillator ensembles with global nonlinear coupling," Physical review letters **98**, 064101 (2007).
[26] A. Pikovsky and M. Rosenblum, "Self-organized partially synchronous dynamics in populations of nonlinearly coupled oscillators," Physica D: Nonlinear Phenomena **238**, 27–37 (2009).
[27] M. Rosenblum and A. Pikovsky, "Two types of quasiperiodic partial synchrony in oscillator ensembles," Physical Review E **92**, 012919 (2015).
[28] A. F. Taylor, M. R. Tinsley, F. Wang, Z. Huang, and K. Showalter, "Dynamical quorum sensing and synchronization in large populations of chemical oscillators," Science **323**, 614–617 (2009).
[29] S. De Monte, F. d'Ovidio, S. Danø, and P. G. Sørensen, "Dynamical quorum sensing: Population density encoded in cellular dynamics," Proceedings of the National Academy of Sciences **104**, 18377–18381 (2007).
[30] J. Zamora-Munt, C. Masoller, J. Garcia-Ojalvo, and R. Roy, "Crowd synchrony and quorum sensing in delay-coupled lasers," Physical review letters **105**, 264101 (2010).
[31] B.-W. Li, C. Fu, H. Zhang, and X. Wang, "Synchronization and quorum sensing in an ensemble of indirectly coupled chaotic oscillators," Physical Review E **86**, 046207 (2012).
[32] D. McMillen, N. Kopell, J. Hasty, and J. Collins, "Synchronizing genetic relaxation oscillators by intercell signaling," Proceedings of the National Academy of Sciences **99**, 679–684 (2002).
[33] J. Garcia-Ojalvo, M. B. Elowitz, and S. H. Strogatz, "Modeling a synthetic multicellular clock: repressilators coupled by quorum sensing," Proceedings of the National Academy of Sciences **101**, 10955–10960 (2004).
[34] E. Ullner, A. Zaikin, E. I. Volkov, and J. García-Ojalvo, "Multistability and clustering in a population of synthetic genetic oscillators via phase-repulsive cell-to-cell communication," Physical review letters **99**, 148103 (2007).
[35] E. Ullner, A. Koseska, J. Kurths, E. Volkov, H. Kantz, and J. García-Ojalvo,

"Multistability of synthetic genetic networks with repressive cell-to-cell communication," Physical Review E **78**, 031904 (2008).

[36]M. B. Elowitz and S. Leibler, "A synthetic oscillatory network of transcriptional regulators," Nature **403**, 335–338 (2000).

[37]E. H. Hellen and E. Volkov, "How to couple identical ring oscillators to get quasiperiodicity, extended chaos, multistability, and the loss of symmetry," Communications in Nonlinear Science and Numerical Simulation **62**, 462–479 (2018).

[38]I. Potapov, B. Zhurov, and E. Volkov, ""quorum sensing" generated multistability and chaos in a synthetic genetic oscillator," Chaos: An Interdisciplinary Journal of Nonlinear Science **22**, 023117 (2012).

[39]E. Sánchez, D. Pazó, and M. A. Matías, "Experimental study of the transitions between synchronous chaos and a periodic rotating wave," Chaos: An Interdisciplinary Journal of Nonlinear Science **16**, 033122 (2006).

[40]P. Perlikowski, S. Yanchuk, M. Wolfrum, A. Stefanski, P. Mosiolek, and T. Kapitaniak, "Routes to complex dynamics in a ring of unidirectionally coupled systems," Chaos: An Interdisciplinary Journal of Nonlinear Science **20**, 013111 (2010).

[41]G. Benettin, L. Galgani, A. Giorgilli, and J.-M. Strelcyn, "Lyapunov characteristic exponents for smooth dynamical systems and for hamiltonian systems; a method for computing all of them. part 1: Theory," Meccanica **15**, 9–20 (1980).

[42]H. Broer, R. Vitolo, and C. Simó, "Quasi-periodic hénon-like attractors in the lorenz-84 climate model with seasonal forcing," in *EQUADIFF 2003* (World Scientific, 2005) pp. 601–606.

[43]A. Kuznetsov, M. Kærn, and N. Kopell, "Synchrony in a population of hysteresis-based genetic oscillators," SIAM Journal on Applied Mathematics **65**, 392–425 (2004).

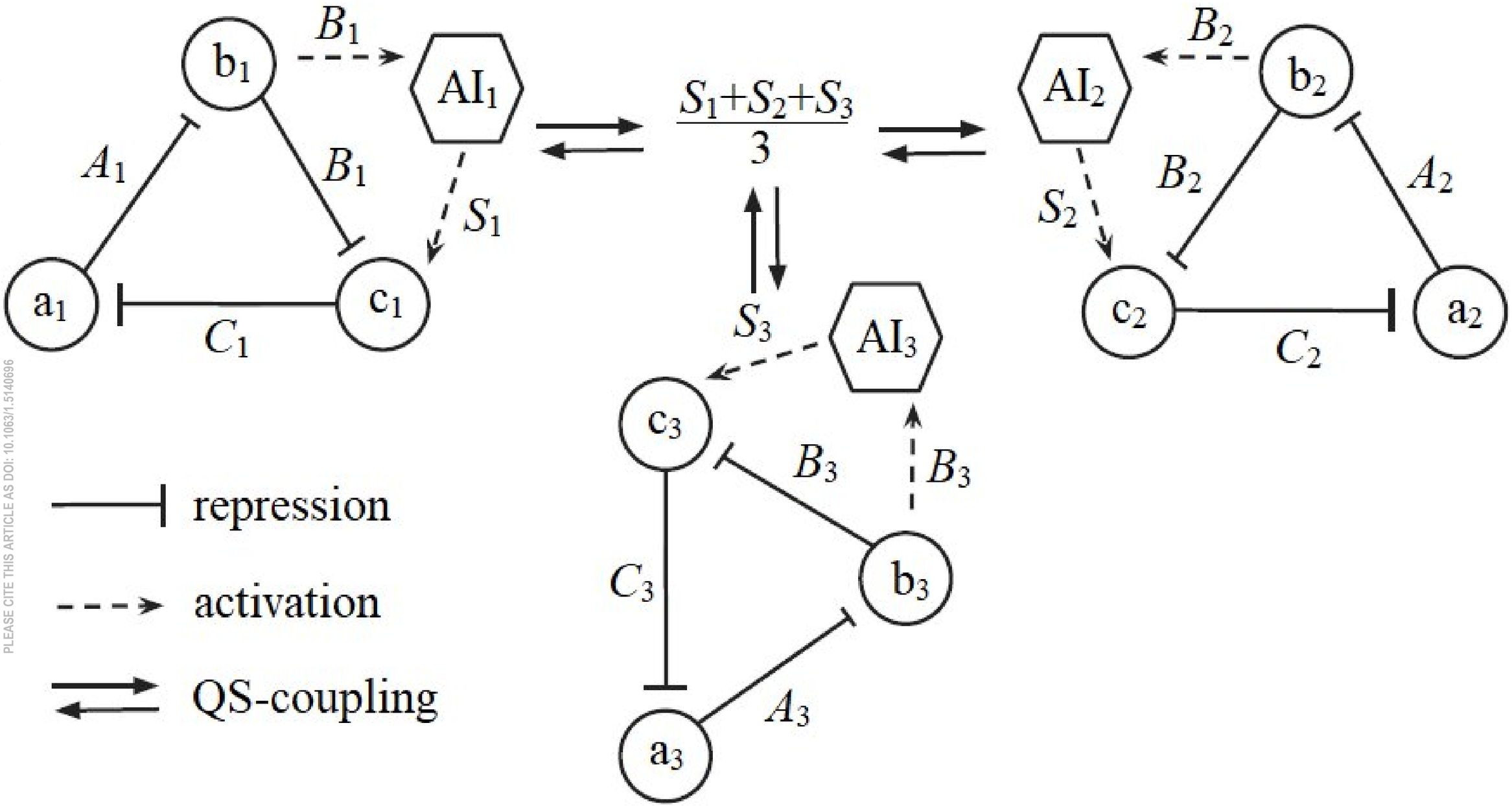

Chaos

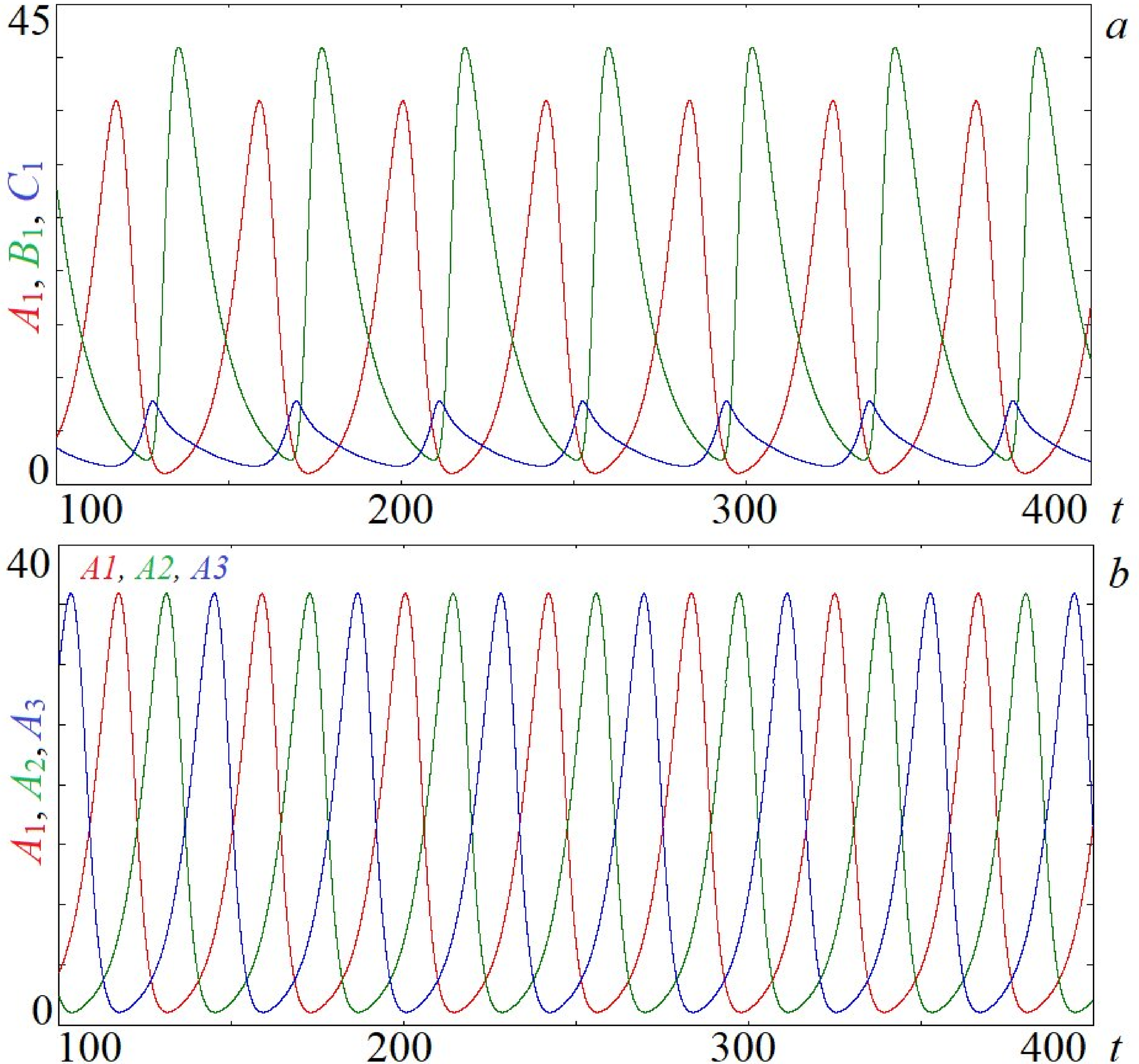

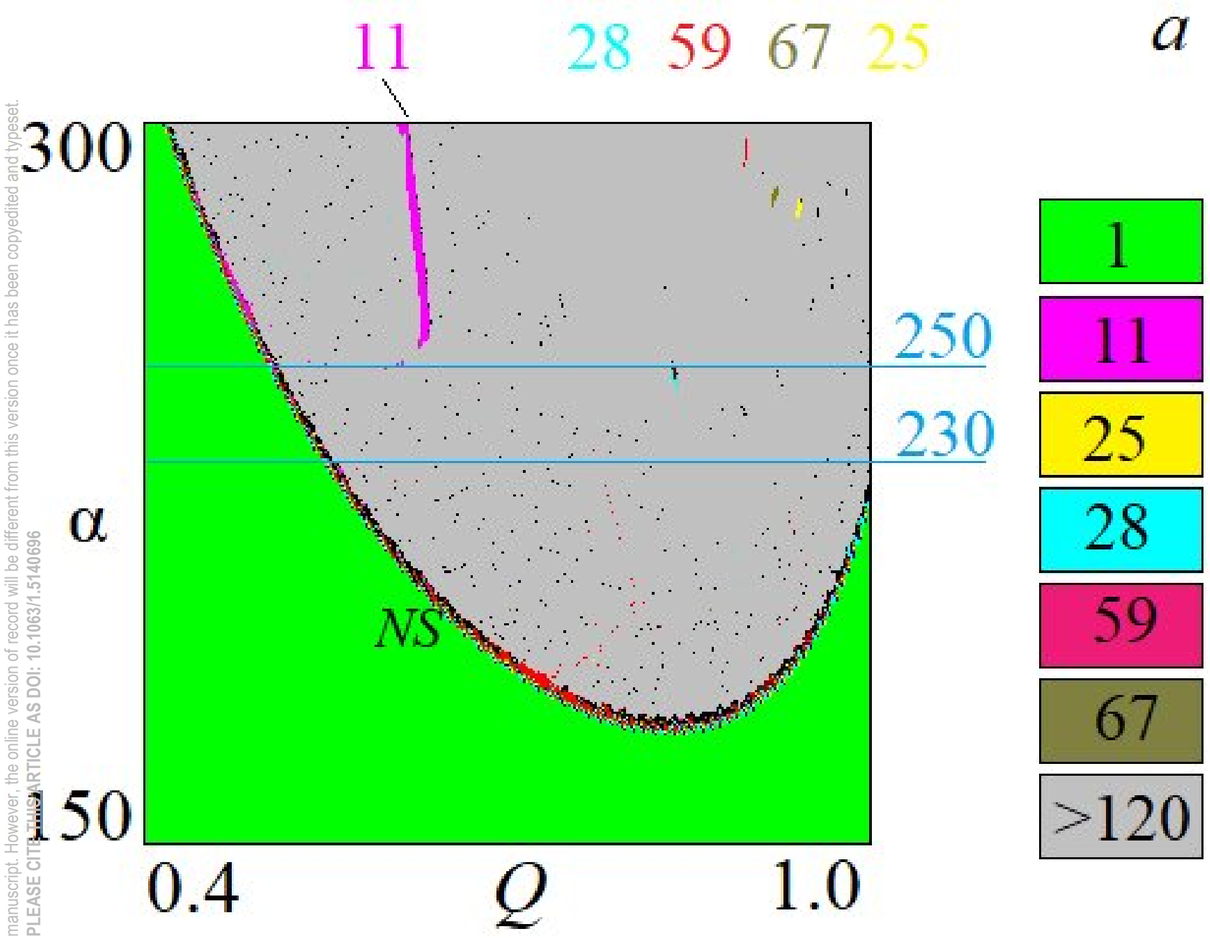

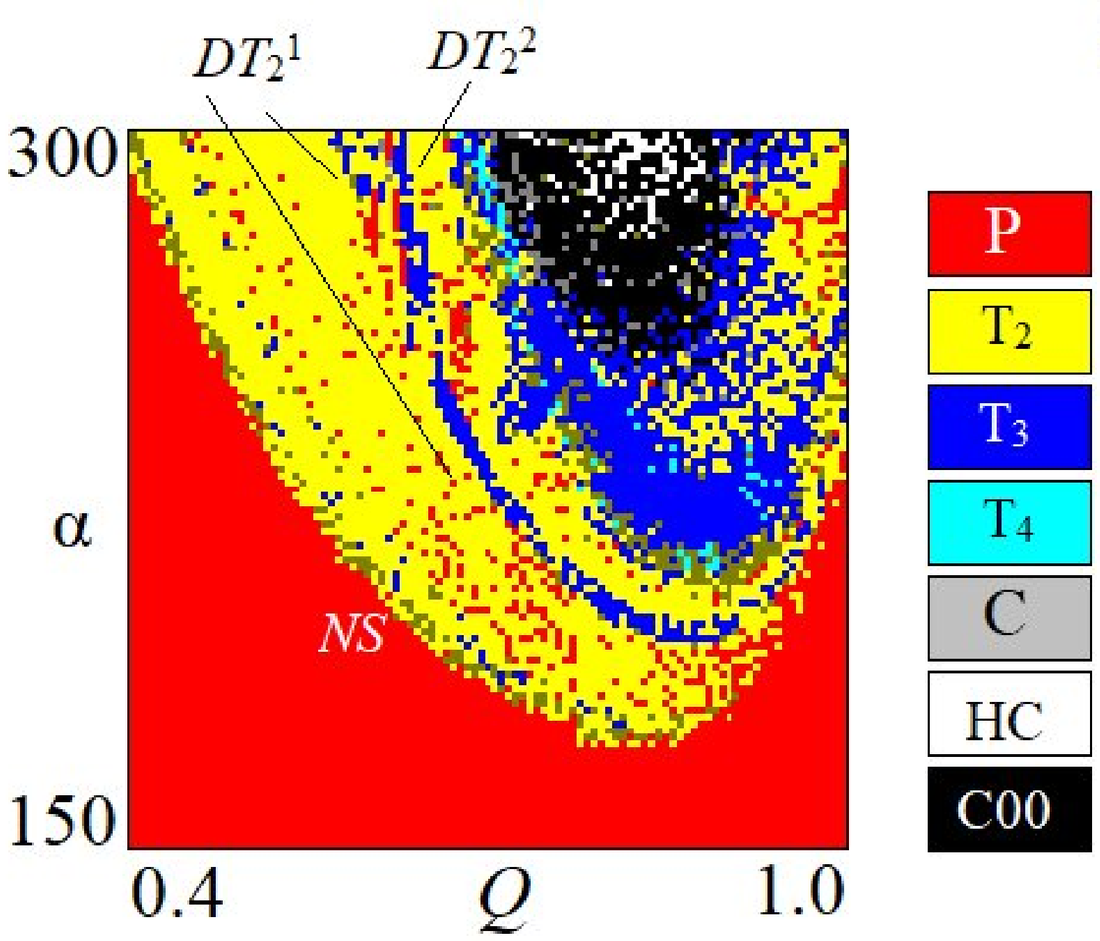

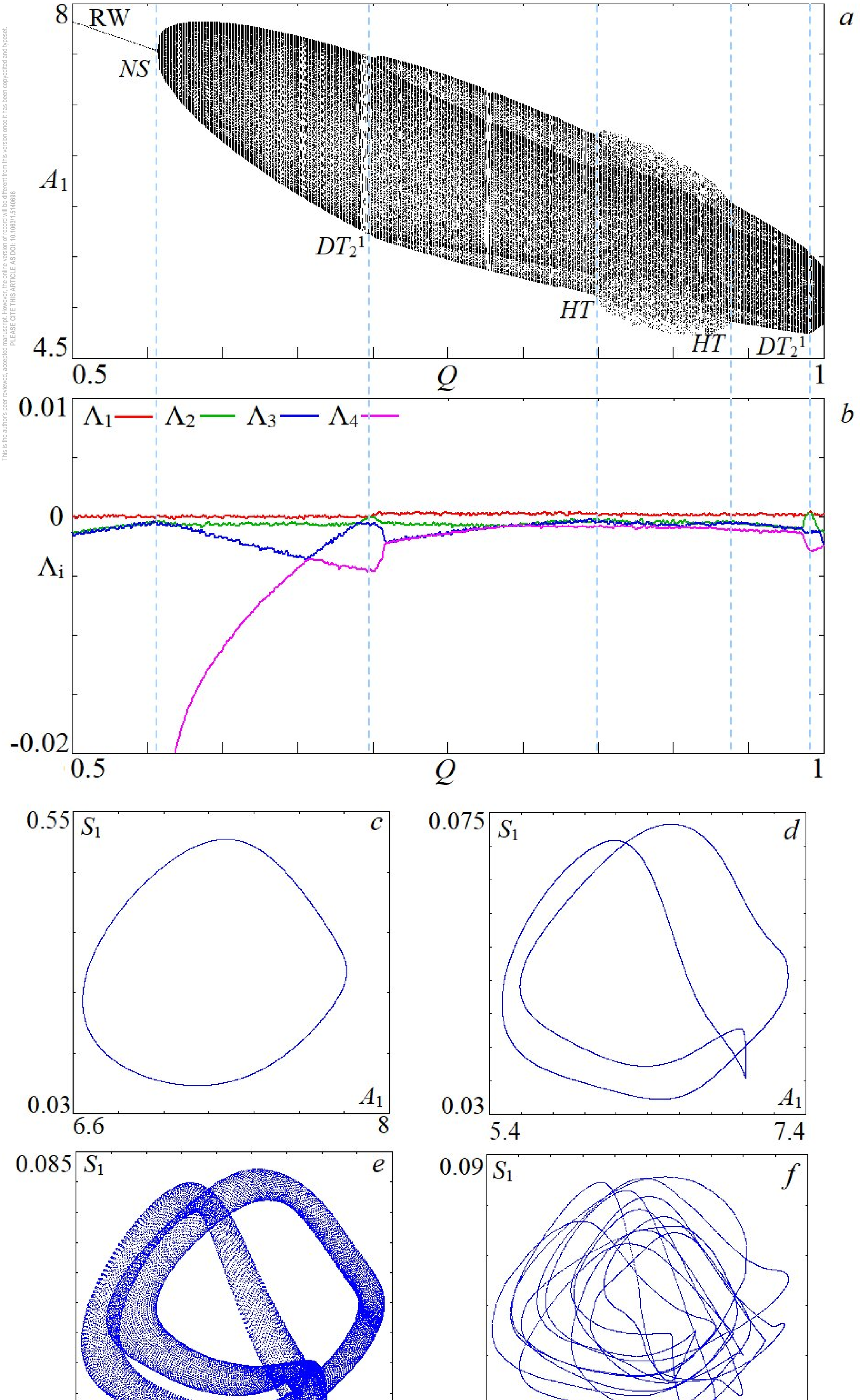

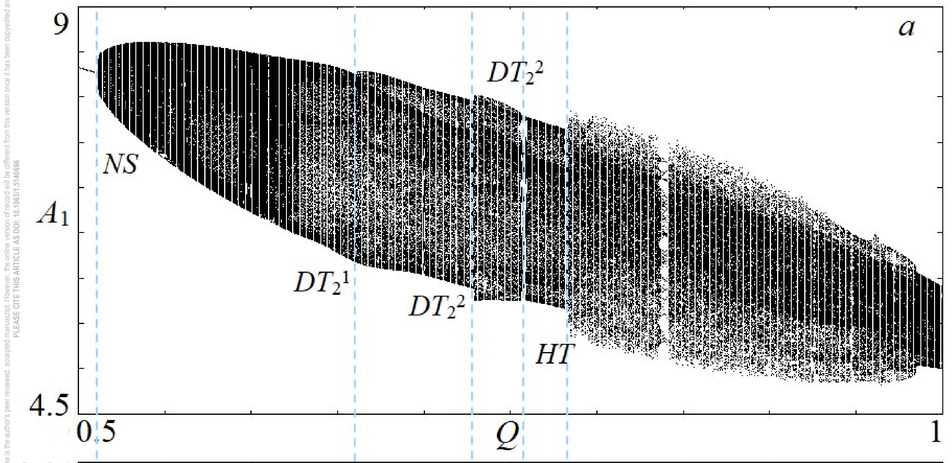

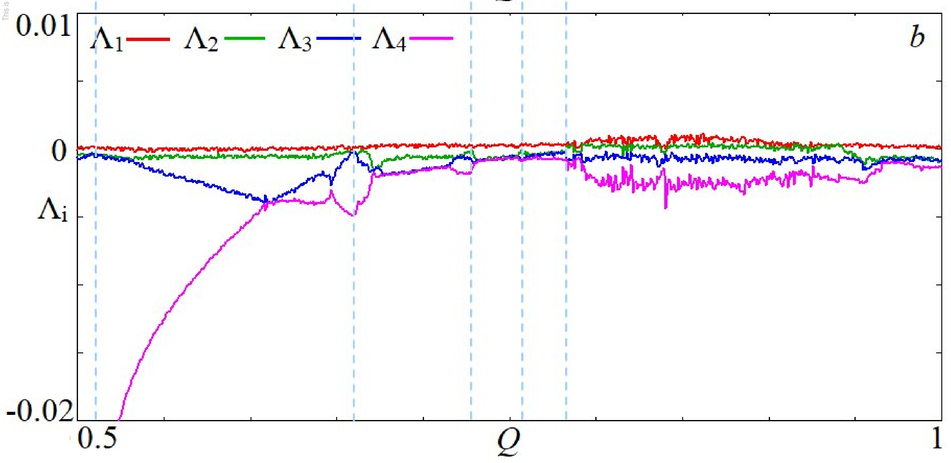

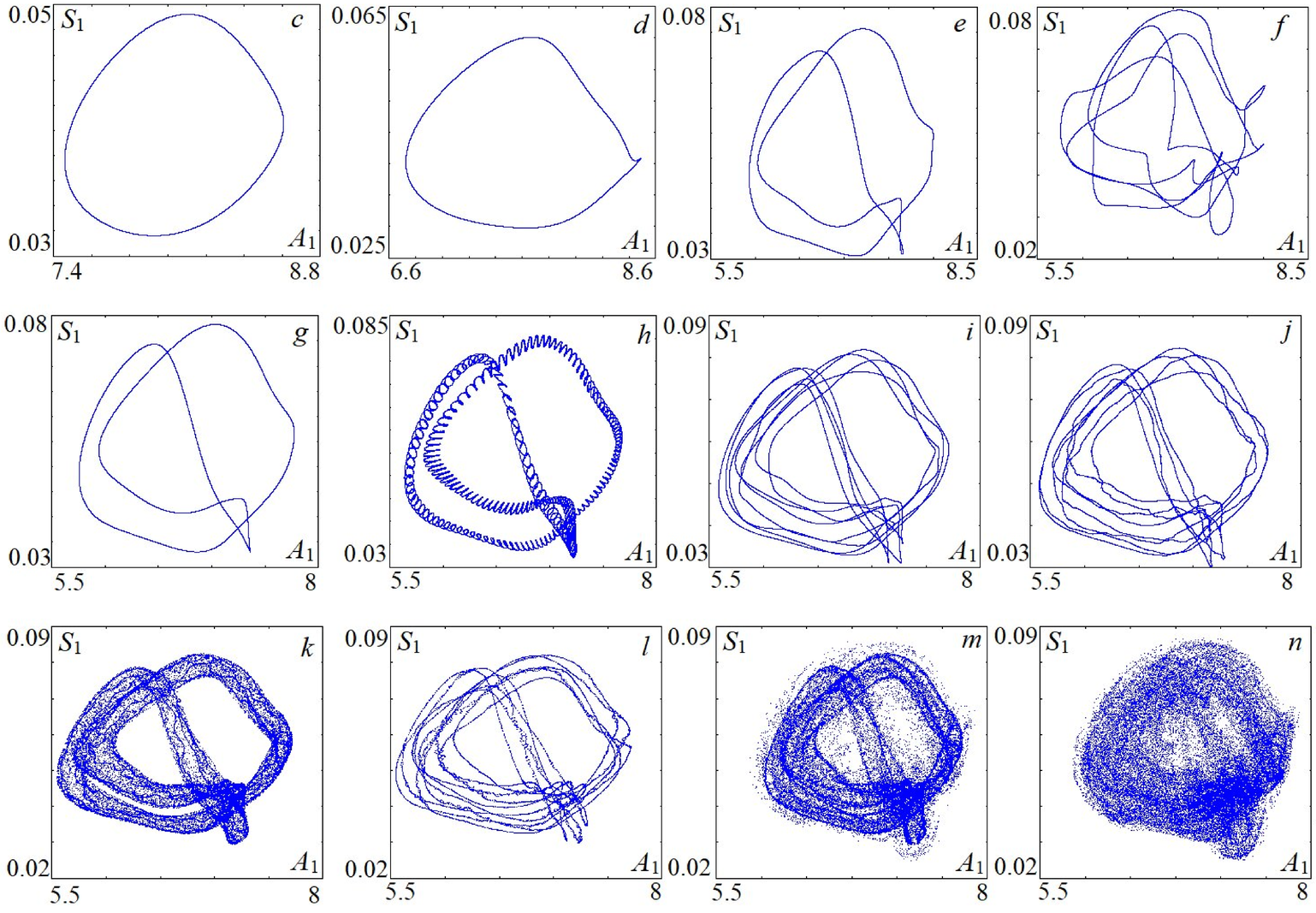

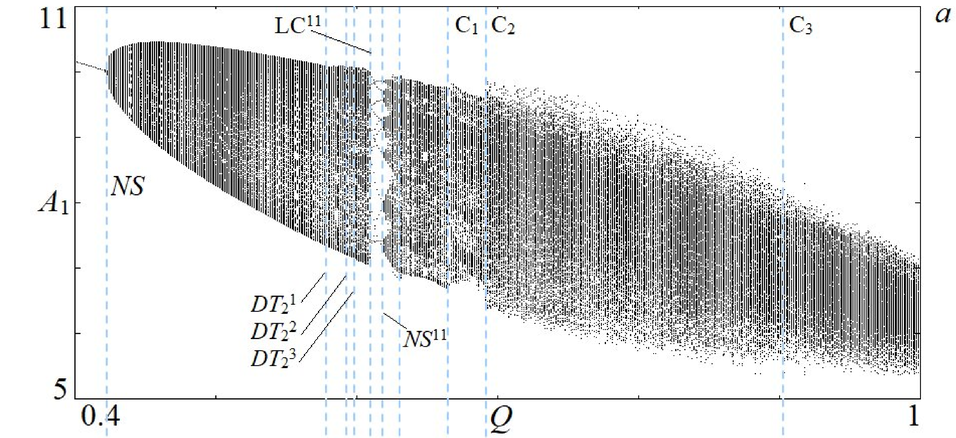

a

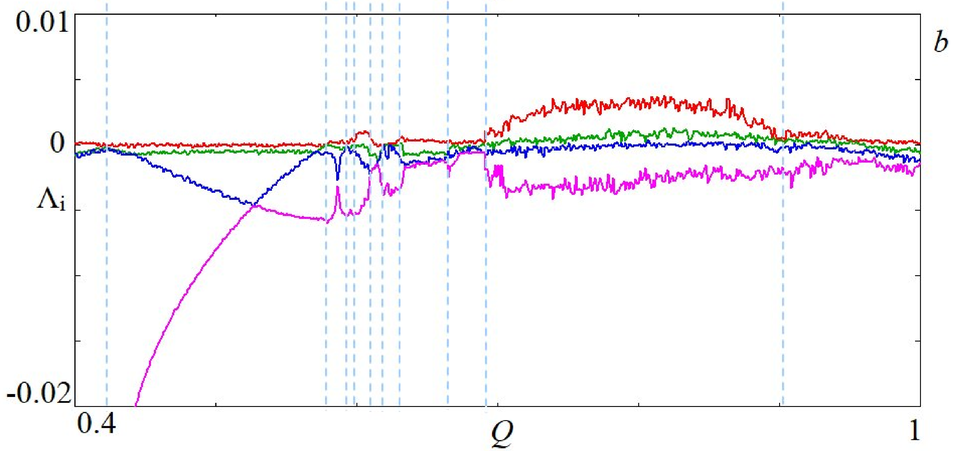

b

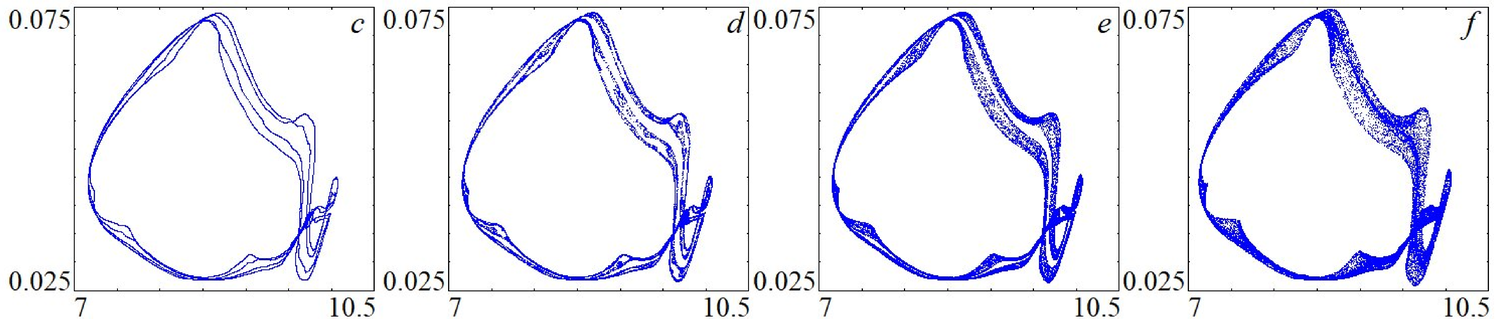

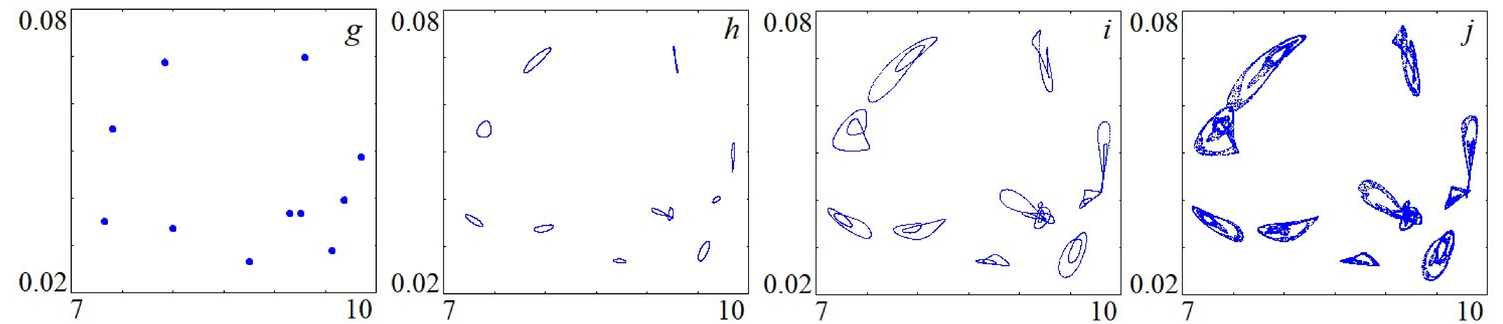

Chaos